INT. J. REMOTE SENSING, 2001, VOL. 22, NO. 10, 1999–2014

A remote sensing–GIS evaluation of urban expansion and its impact on surface temperature in the Zhujiang Delta, China

Q. WENG

Department of Geography, University of Alabama, Tuscaloosa, AL 35487, USA

(*Received 26 May 1999; in final form 22 November 1999*)

Abstract. The Zhujiang Delta of South China has experienced a rapid urban expansion over the past two decades due to accelerated economic growth. This paper reports an investigation into the application of the integration of remote sensing and geographic information systems (GIS) for detecting urban growth and assessing its impact on surface temperature in the region. Remote sensing techniques were used to carry out land use/cover change detection by using multitemporal Landsat Thematic Mapper data. Urban growth patterns were analysed by using a GIS-based modelling approach. The integration of remote sensing and GIS was further applied to examine the impact of urban growth on surface temperatures. The results revealed a notable and uneven urban growth in the study area. This urban development had raised surface radiant temperature by 13.01 K in the urbanized area. The integration of remote sensing and GIS was found to be effective in monitoring and analysing urban growth patterns, and in evaluating urbanization impact on surface temperature.

1. Introduction

Land covers, as the biophysical state of the earth's surface and immediate subsurface, are sources and sinks for most of the material and energy movements and interactions between the geosphere and biosphere. Changes in land cover include changes in biotic diversity, actual and potential primary productivity, soil quality, runoff, and sedimentation rates (Steffen *et al.* 1992), and cannot be well understood without the knowledge of land use change that drives them. Therefore, land use and land cover changes have environmental implications at local and regional levels, and perhaps are linked to the global environmental process. Because of the interrelated nature of the elements of the natural environment, the direct effects on one element may cause indirect effects on others.

Urbanization, the conversion of other types of land to uses associated with growth of populations and economy, is a main type of land use and land cover change in human history. It has a great impact on climate. By covering with buildings, roads and other impervious surfaces, urban areas generally have a higher solar radiation absorption, and a greater thermal capacity and conductivity, so that heat is stored during the day and released by night. Therefore, urban areas tend to experience a relatively higher temperature compared with the surrounding rural areas. This thermal difference, in conjunction with waste heat released from urban houses, transportation and industry, contribute to the development of urban heat

International Journal of Remote Sensing
ISSN 0143-1161 print/ISSN 1366-5901 online
http://www.tandf.co.uk/journals

island (UHI). The temperature difference between the urban and the rural areas are usually modest, averaging less than 1° C, but occasionally rising to several degrees when urban, topographical and meteorological conditions are favourable for the UHI to develop (Mather 1986).

In China, land use and land cover patterns have undergone a fundamental change due to accelerated economic development under its economic reform policies since 1978. Urban growth has been speeded up, and extreme stress to the environment has occurred. This is particularly true in the coastal region such as the Zhujiang Delta where massive agricultural land is disappearing each year, converting to urban or related uses. Evaluating the magnitude and pattern of China's urban growth is an urgent need. Furthermore, because of the lack of appropriate land use planning and the measures for sustainable development, rampant urban growth has been creating severe environmental consequences. Thus, there also is a need to assess the environmental impact of the rapid urban expansion.

The integration of remote sensing and geographic information systems (GIS) has been widely applied and been recognized as a powerful and effective tool in detecting urban land use and land cover change (Ehlers *et al.* 1990, Treitz *et al.* 1992, Harris and Ventura 1995). Satellite remote sensing collects multispectral, multiresolution and multitemporal data, and turns them into information valuable for understanding and monitoring urban land processes and for building urban land cover datasets. GIS technology provides a flexible environment for entering, analysing and displaying digital data from various sources necessary for urban feature identification, change detection and database development. However, few of the urban growth studies has linked to post-change detection environmental impact analysis. The question of how to develop an operational procedure using the existing techniques of remote sensing and GIS for examining environmental impacts of rapid urban growth remains to be answered.

The goal of this paper is to demonstrate the integrated use of remote sensing and GIS in addressing environmental issues in China at a local level. Specific objectives are to evaluate urban growth patterns in the Zhujiang Delta and to analyse the impact of the urban growth on surface temperature.

2. Study area

The study area, the Zhujiang (literally 'the Pearl River') Delta, is located between latitudes 21° 40′ N and 23° N, and longitudes 112° E and 113° 20′ E (figures 1 and 2). It is the third biggest river delta in China and has an area of 17 200 km^2. Because of the constraint of satellite data coverage, this research focuses on the core area of the delta that includes the following 15 cities/counties: Guangzhou, Panyu, Sanshui, Nanhai, Foshan, Shunde, Jiangmen, Zhongshan, Zhuhai, Xinhui, Doumen, Zengcheng, Dongguan, Baoan and Shenzhen. Geomorphologically, the Zhujiang Delta consists of three sub-deltas formed by sediments, the Xijiang, Beijiang and Donjiang Deltas, originated approximately 40 thousand years ago (Department of Geography, Zhongshan University 1988). The process of sedimentation still continues today, extending seaward at a rate of 40 m per year (Gong and Chen 1964). The delta has a subtropical climate with an average annual temperature between 21 and 23° C, and an average precipitation ranging from 1600 to 2600 mm. Because of the impact of the East Asian Moonsoonal circulation, about 80% of the rainfall comes in the period of April to September with a concentration in the months of May to July, when flooding is prone to occur (Ditu Chubanshe 1977). Another

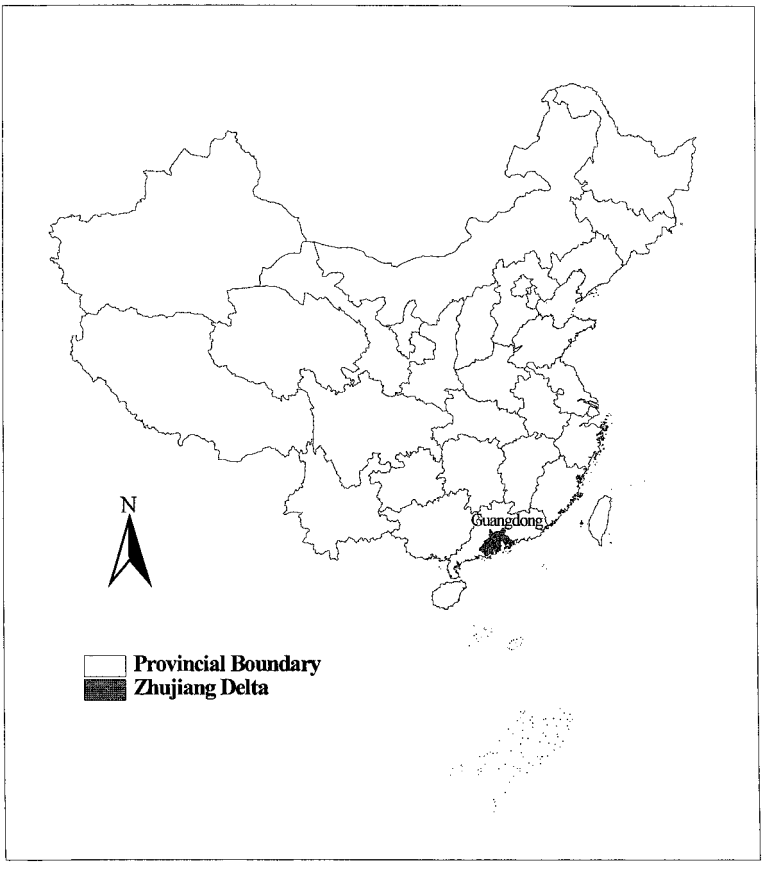

Figure 1. A map of the study area.

hazard is typhoons, which occur most frequently from June to October. The delta's fertile alluvial deposits, in combination with the subtropical climate, make it one of the richest agricultural areas in China. The famous dike–pond ecological agricultural systems and silk production can be traced back to the beginning of the Ming Dynasty (1368–1644 A.D.) (Zhong 1980, Ruddle and Zhong 1988).

Economically, the Zhujiang Delta is the largest area of economic concentration in South China. Guangzhou, China's sixth largest city, Hong Kong and Macao are located here. Since 1978, the delta has become a rising star due to its dramatic economic expansion under China's economic reform policies, and therefore has been regarded as a model for Chinese regional development. The establishment of Shenzhen and Zhuhai Special Economic Zones in 1979 and the Zhujiang Delta Economic Open Zone in 1985 has stimulated Hong Kong and foreign firms to locate their factories there as village–township enterprises. The labour-intensive industries, in association with the cash crop production, notably, seafood, poultry, vegetables, fruit and flowers, have transformed the spatial economy of the delta (Lo 1989, Weng 1998). The rapid economic development has brought about fundamental changes in land use and land cover patterns. The integrated approach developed in this paper is to analyse the changing patterns of urban land use/cover and its impact on surface temperature.

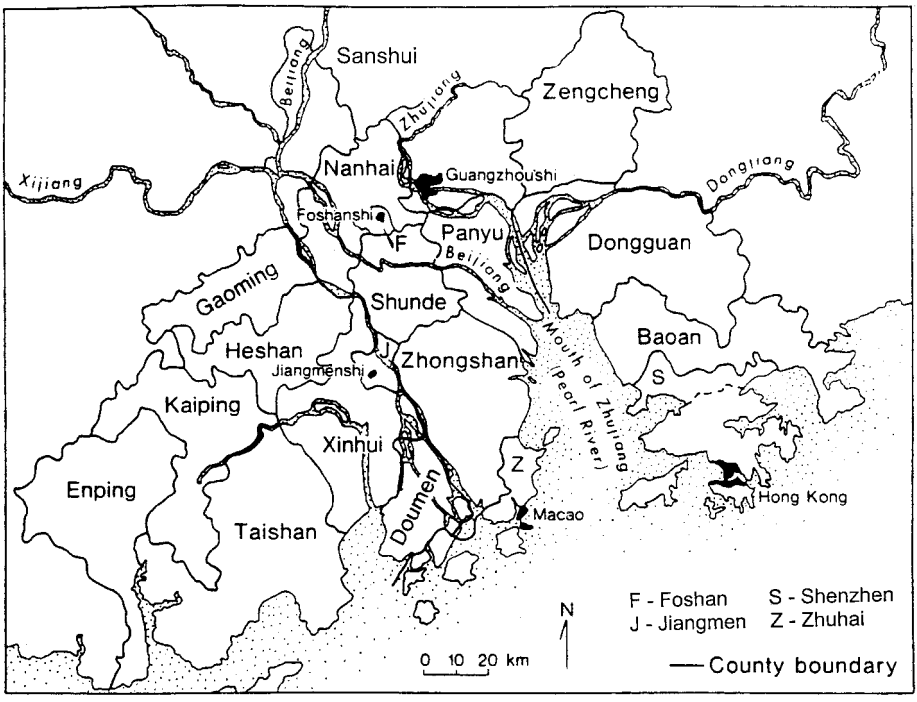

Figure 2. Major rivers, counties and cities in the Zhujiang Delta (after Lo 1989).

3. Methodology

3.1. *Urban expansion detection and analysis*

Land use/cover patterns for 1989 and 1997 were mapped by the use of Landsat Thematic Mapper (TM) data (Dates: 13 December 1989 and 29 August 1997). Seven land use and land cover types are identified and used in this study, including: (1) urban or built-up land, (2) barren land, (3) cropland, (4) horticulture farms, (5) dike–pond land, (6) forest, and (7) water. With the aid of Erdas Imagine computer software, each Landsat image was enhanced using histogram equalization (in order to gain a higher contrast in the 'peaks' of the original histogram) to increase the volume of visible information. This procedure is important for helping identify ground control points in rectification. All images are rectified to a common UTM (Universal Transverse Mercator) coordinate system based on the 1550 000 topographic maps of Guangdong Province produced by the Chinese government. Each image was then radiometrically corrected using relative radiometric correction method (Jensen 1996). A supervised classification with the maximum likelihood algorithm was conducted to classify the Landsat images using bands 2 (green), 3 (red) and 4 (near-infrared). The accuracy of the classification was verified by field checking or comparing with existing land use and cover maps that have been field-checked.

In performing land use/cover change detection, a cross-tabulation detection method was employed. A change matrix was produced with the help of Erdas Imagine software. Quantitative areal data of the overall land use/cover changes as well as gains and losses in each category between 1989 and 1997 were then compiled. In order to analyse the nature, rate, and location of urban land change, an image of urban and built-up land was extracted from each original land cover image. The

extracted images were then overlaid and recoded to obtain an urban land change (expansion) image.

The urban expansion image was further overlaid with several geographic reference images to help analyse the patterns of urban expansion, including an image of the county/city boundary, major roads, and major urban centres. These layers were constructed in a vector GIS environment and converted into a raster format (grid size = 30 m). The county/city boundary image can be utilized to find urban land change information within each county/city. Because proximity to a certain object, such as major roads, has an important implication in urban land development, urban expansion processes often show an intimate relationship with distance from these geographic objects. Using the buffer function in GIS, a buffer image was generated, showing the proximity to the major roads of the study area. Ten buffer zones were created around a major road with a width of 500 m. Local conditions have been taken into account in selecting these buffer widths. The buffer image was overlaid with the urban expansion image to calculate the amount of urban expansion in each zone. The density of urban expansion was then calculated by dividing the amount of urban expansion by the total amount of land in each buffer zone. These values of density can be used to construct a distance decay function of urban expansion.

3.2. *Urbanization expansion impact analysis*

Urban development usually gives rise to a dramatic change of the Earth's surface, as natural vegetation is removed and replaced by non-evaporating and non-transpiring surfaces such as metal, asphalt and concrete. This alteration will inevitably result in the redistribution of incoming solar radiation, and induce the urban–rural contrast in surface radiance and air temperature. The difference in ambient air temperature between an urban and its surrounding rural area is known as the effect of UHI. Given the relationship between surface radiant temperature and the texture of land cover, the impact of urban development on surface temperature in the Zhujiang Delta can be assessed.

Studies on surface temperature characteristics of urban areas using satellite remote sensing data have been conducted primarily using NOAA AVHRR data (Kidder and Wu 1987, Balling and Brazell 1988, Roth *et al.* 1989, Gallo *et al.* 1993a). The 1.1 km spatial resolution of these data are found suitable only for small-scale urban temperature mapping. The much higher resolution (120 m) Landsat TM thermal infrared data were seldom used to derive surface temperature. Recently, Carnahan and Larson (1990) have used the TM thermal infrared data to observe mesoscale temperature differences between urban and rural areas in Indianapolis, while Nichol (1994) used it to monitor microclimate for some housing estates in Singapore. However, no research has yet attempted to detect urban-induced surface temperature change over time at a local level using multidate TM thermal infrared data.

To measure the surface temperature change from 1989 to 1997, surface radiant temperatures were derived from radiometrically corrected TM thermal infrared data (band 6), using the following quadratic model to convert the digital number (DN) into radiant temperatures (Malaret *et al.* 1985):

$$T(\mathrm{K}) = 209.831 + 0.834\,\mathrm{DN} - 0.00133\,\mathrm{DN}^2 \quad (1)$$

Then, corrections for emissivity (ε) were applied to the radiant temperatures according to the nature of land cover. In general, vegetated areas were given a value of 0.95

and non-vegetated areas 0.92 (Nichol 1994). The emissivity corrected surface temperature can be computed as follows (Artis and Carnahan 1982):

$$T_s = \frac{T(\mathrm{K})}{1 + (\lambda T(\mathrm{K})/\alpha)\ln \varepsilon} \tag{2}$$

where λ = wavelength of emitted radiance (for which the peak response and the average of the limiting wavelengths ($\lambda = 11.5\ \mu$m) (Markham and Barker 1985) will be used), $\alpha = hc/K$ (1.438×10^{-2} mK), K = Stefan Boltzmann's constant (1.38×10^{-23} J K^{-1}), h = Planck's constant (6.26×10^{-34} J s), and c = velocity of light (2.998×10^{8} s^{-1}).

In examining the spatial relationship between land use/cover types and the surface energy response as measured by T_s, the classified land cover images in 1989 and 1997 were overlaid to the T_s image of corresponding years. Because normalized difference vegetation index (NDVI) has been found to be a good indicator of surface radiant temperature (Nemani and Running 1989, Gallo *et al.* 1993b, Gillies and Carlson 1995, Lo *et al.* 1997), a NDVI image was computed for 1989 and 1997 from visible (0.63–0.69 μm) and near-infrared (0.76–0.90 μm) data of the Landsat TM, using the following formula:

$$\mathrm{NDVI} = \frac{\mathrm{TM}_4 - \mathrm{TM}_3}{\mathrm{TM}_4 + \mathrm{TM}_3} \tag{3}$$

The resultant NDVI image was overlaid with the T_s image for each year. In this way, the interactions among land use/cover, NDVI, and surface temperature can be revealed.

Surface temperature change image between 1989 and 1997 was also produced using image differencing. This image was overlaid with the land use/cover change map and with the NDVI change map to study how all these changes have interacted.

4. Results and discussion

4.1. *Urban expansion in the Zhujiang Delta, 1989–1997*

The overall accuracy of the land use/cover map for 1989 and 1997 were determined to be 90.57% and 85.43%, respectively (tables 1 and 2). The Kappa indices for the 1989 and 1997 maps were 0.8905 and 0.8317, respectively. Clearly, these data have reasonably high accuracy, and thus are sufficient for urban growth detection.

Table 3 shows the land use and land cover change matrix of the Zhujiang Delta from 1989 to 1997. From this table, it is clear that there has been a considerable change (12.82% of the total area) in land use and land cover in the study area during the 8-year period. Urban or built-up land and horticulture farms have increased in area (by 47.68% and 88.66%, respectively), and cropland has decreased in area (by 48.37%).

The overlay of the 1989 and 1997 land use/cover map further indicates that of the 47.68% (65 690 ha) increase in urban or built-up land, most results from cropland (37.92%) and horticulture farms (16.05%). Figure 3 shows the areal extent and spatial occurrence of the urban expansion. The overlay of this map with a city–county mask reveals the spatial occurrence of urban expansion within administrative regions. Table 4 shows that in absolute term the greatest urban expansion occurred in Dongguan (23 478.90 ha), Baoan (14 941.08 ha), Nanhai (8004.1 ha) and Zhuhai (5869.71 ha). However, in percentage terms, the largest increase in urban or built-up land occurred in Zhuhai (1100.00%), followed by Shenzhen (306.65%), Baoan

Table 1. Error matrix of the land use and land cover map, 1989.

Classified data	Reference data								RT	CT	PA (%)	UA (%)
	UC	UB	BL	CR	HF	DP	FO	WA				
UC	0	0	0	0	0	0	0	0	7	0		
UB	0	48	0	0	2	0	0	0	48	50	100	96.0
BL	6	0	44	0	0	0	0	0	44	50	100	88.0
CR	1	0	0	42	4	1	2	0	45	50	93.3	84.0
HF	0	0	0	1	45	0	4	0	54	50	83.3	90.0
DP	0	0	0	2	1	42	0	5	43	50	97.7	84.0
FO	0	0	0	0	2	0	47	1	54	50	87.0	94.0
WA	0	0	0	0	0	0	1	49	55	50	89.1	98.0
Column total	7	48	44	45	54	43	54	55				
Overall accuracy		90.57%										

UC, Unclassified; UB, urban or built-up land; BL, barren land; CR, crop land; HF, horticulture farm; DP, dike–pond land; FO, forest; WA, water.

RT, Reference total; CT, classified total; PA, producer's accuracy; UA, user's accuracy.

Table 2. Error matrix of the land use and land cover map, 1997.

Classified data	Reference data								RT	CT	PA (%)	UA (%)
	UC	UB	BL	CR	HF	DP	FO	WA				
UC	0	0	0	0	0	0	0	0	21	0		
UB	1	42	2	0	5	0	0	0	42	50	100	84.0
BL	20	0	30	0	0	0	0	0	32	50	93.8	60.0
CR	0	0	0	38	11	0	1	0	40	50	95.0	76.0
HF	0	0	0	2	47	1	0	0	65	50	72.3	94.0
DP	0	0	0	0	2	43	0	5	44	50	97.7	86.0
FO	0	0	0	0	0	0	49	1	50	50	98.0	98.0
WA	0	0	0	0	0	0	0	50	56	50	89.3	100
Column total	21	42	32	40	65	44	50	56				
Overall accuracy		85.43%										

UC, Unclassified; UB, urban or built-up land; BL, barren land; CR, crop land; HF, horticulture farm; DP, dike–pond land; FO, forest; WA, water.

RT, Reference total; CT, classified total; PA, producer's accuracy; UA, user's accuracy.

(233.33%) and Dongguan (125.71%). Massive urban sprawl in these areas can be ascribable to rural urbanization, which is a common phenomenon in the post-reform China. Rapid urban development in the form of small towns in the east side of the delta is highly influenced by the investment from Hong Kong (Yeh and Li 1996). In contrast, those old cities, such as Guangzhou and Foshan, do not show a rapid increase in urban or built-up land because they have no land to expand further (as they have already expanded fully in the past) and the concentration of urban enterprises in the city proper. Shenzhen and Zhuhai were designated as Special Economic Zones at the same time, but the pace of urbanization in the two cities is quite different. Urban development in Shenzhen has mostly been completed in the

Table 3. Land use/cover change matrix, 1989–1997 (ha).

	1997								
1989	Unclassified	Urban or built-up	Barren land	Cropland	Horticulture farms	Dike-pond land	Forest	Water	1989 Total
Unclassified	3 918 240	0	0	0	0	0	0	0	3 918 240
Urban or built-up	0	54 189	493.38	208 90.8	35 816.8	15 887.4	3082.77	7407.36	13 7768
Barren land	0	11 603.4	661.77	4156.02	8690.4	1285.47	1414.53	1293.75	29 105.4
Cropland	0	77 151.5	4651.11	152 400	215 536	55 272.7	44 497.1	29 258.4	578 767
Horticulture farms	0	32 660.8	3775.23	44 972.9	132 372	12 850.2	43 752.3	8222.22	278 605
Dike–pond land	0	14 902.8	321.03	33 931.4	20 238.6	42 489.7	2640.96	31 327.4	145 852
Forest	0	8378.64	3028.59	26 294.7	102 589	3906.72	128 048	5436.81	277 683
Water	0	4571.37	472.95	16 156.6	10 366.1	11 179.7	1845.09	64 414.3	109 006
1997 Total	3 918 240	203 458	13 404.1	29 8803	525 609	142 872	225 281	147 360	5 475 026.88
Change (ha)	0	65 690	−15 701.3	−279 964	247 004	−2980	−52 402	38 354	702 095.3
Change (%)	0	+47.68	−53.93	−48.37	+88.66	−0.02	−18.87	+3.19	12.82

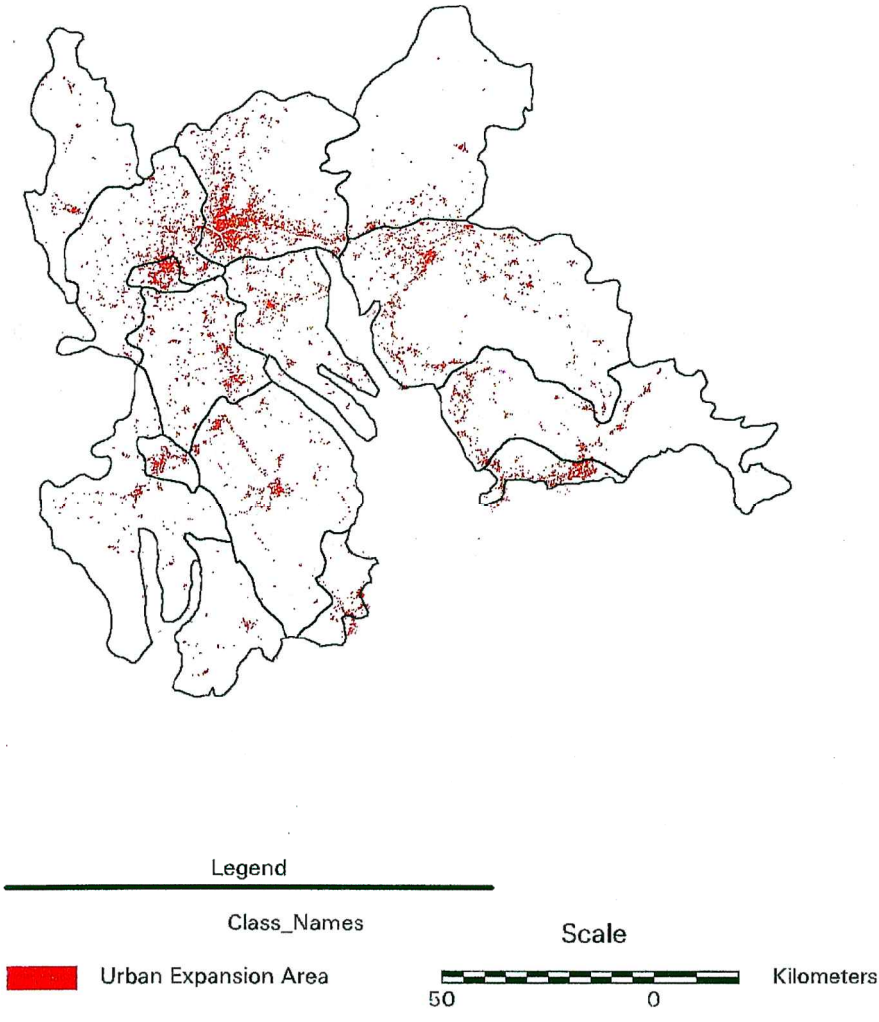

Figure 3. A map or urban expansion in the Zhujiang Delta, 1989–1997.

1980s, while Zhuhai's urban expansion appears primarily during the period of 1989–1997 (5869.71 ha).

Urban expansion processes in the Zhujiang Delta during the period of 1989 to 1997 are further examined by plotting a distance decay curve from a major road, and establishing a mathematical equation. The result indicates that the density of urban expansion decreases as the distance increases away from a major road. Most urban expansion (66%) can be observed within a distance of 2000 m from a major road. This rapid urban expansion pattern is vividly illustrated along the superhighway from Guangzhou to Hong Kong as seen in figure 3, where Hong Kong investors seek sites for constructing factories and housing. The relationship between the density of urban expansion (Y) and the distance from a major road (X) can be mathematically expressed as:

$$Y = 0.2237\, e^{-0.00046x} \quad (4)$$

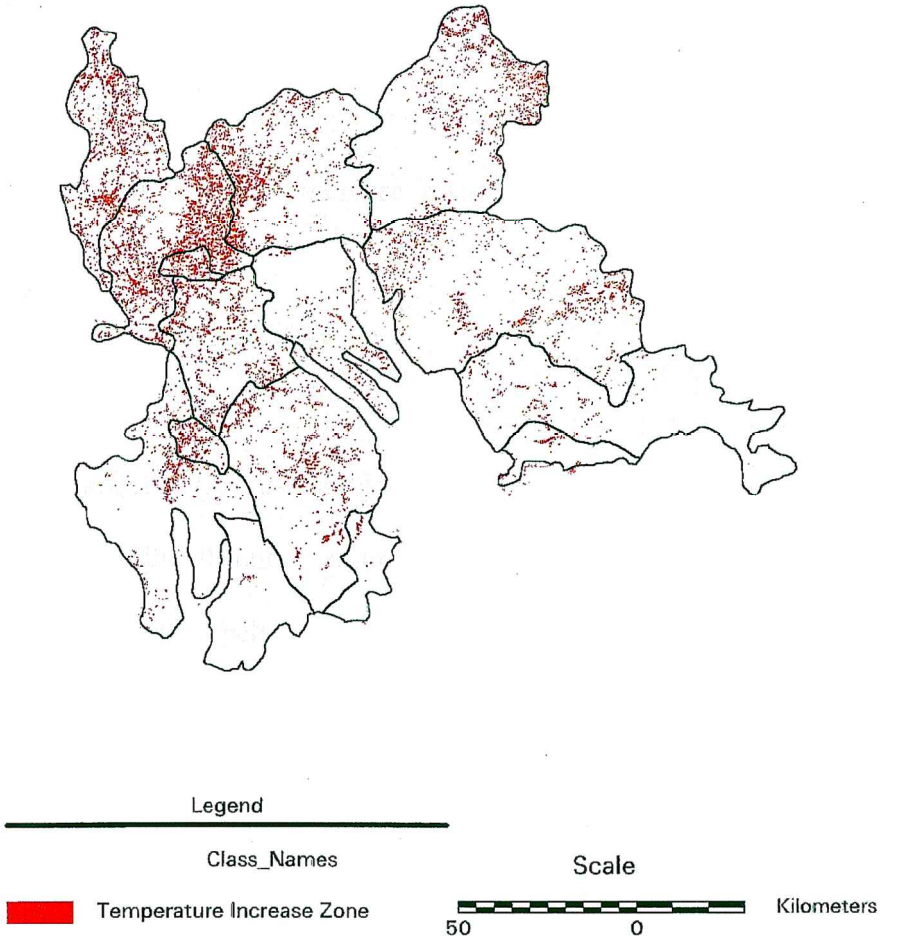

Figure 4. Spatial distribution of temperature increase zones, 1989–1997.

4.2. *Urbanization impact on surface temperature*

4.2.1. *Thermal signatures of land cover types*

In order to understand the impacts of land use/cover change on surface radiant temperature, the characteristics of the thermal signatures of each land cover type must be studied first. The average values of radiant surface temperatures by land cover type in 1989 and 1997 are summarized in table 5. It is clear that for both years, urban or built-up land exhibits the highest surface radiant temperature (336.30 K in 1989 and 339.14 K in 1997), followed by barren land (335.52 K in 1989 and 338.36 K in 1997). This implies that urban development does bring up surface radiant temperature by replacing natural vegetation with non-evaporating, non-transpiring surfaces such as stone, metal and concrete. The standard deviations of the radiant temperature values are small for both land cover types, indicating that urban surfaces do not experience a wide variation in surface radiant temperature because of the dry nature of non-evapotranspirative urban materials. The lowest radiant temperature in 1989 is observed in forest (308.83 K), followed by water bodies (309.76 K), dike–pond land (312.39 K) and cropland (314.36 K). This pattern

Table 4. Satellite-detected urban expansion in the Zhujiang Delta, 1989–1997.

City/county	Urban area 1989 (ha)	Urban area 1997 (ha)	Change (ha)	Change (%)
Baoan	6403.32	21 344.40	14 941.08	233.33
Dongguan	18 676.3	42 155.20	23 478.90	125.71
Doumen	2134.44	3735.27	1600.83	75.00
Foshan	6403.32	6936.93	533.61	8.33
Guangzhou	23 478.8	28 281.30	4802.50	20.45
Jiangmen	1600.83	3735.27	2134.44	133.33
Nanhai	13 340.3	21 344.40	8004.10	60.00
Panyu	7470.54	8537.76	1067.22	14.29
Sanshui	2134.44	2134.44	0.00	0.00
Shenzhen	1049.76	4268.88	3219.12	306.65
Shunde	6403.32	10 138.60	3735.28	58.33
Xinhui	5869.71	7470.54	1601.44	27.27
Zengcheng	5869.71	5869.71	0.00	0.00
Zhongshan	13 340.30	16 541.90	3201.60	24.00
Zhuhai	533.61	6403.32	5869.71	1100.00

Table 5. Average surface temperature in degrees Kelvin by land cover type.

Land cover	1989	Standard deviation (±)	1997	Standard deviation (±)
Urban or built-up land	336.30	7.27	339.14	8.38
Barren land	335.52	6.57	338.36	6.80
Cropland	314.36	9.14	316.63	11.02
Horticulture farms	315.60	14.90	317.84	15.03
Dike–pond land	312.39	4.70	314.83	4.85
Forest	308.83	10.64	312.91	10.29
Water	309.76	9.37	311.05	10.04

is in contrast with that in 1997, when the low radiant temperature is found in water bodies (311.05 K), followed by forest (312.91 K), dike–pond land (314.83 K) and cropland (316.63 K). This different pattern is primarily attributed to the differences in solar illumination, the state of vegetation, and atmospheric influences on the remotely sensed TM dataset. The 1989 image was taken in winter (13 December) while the 1997 image in summer (27 August). The difference in data acquisition season is clearly reflected in the surface radiant temperatures of water bodies. The radiant temperature of water bodies is higher than that of forest by 0.83 K in winter, while in summer lower than that of forest by 1.86 K. Because of distinctive characteristics of rivers, lakes, and oceans, their radiant temperature values vary. Rivers (315.12 K) and lakes (314.33 K) register a much higher temperature than oceans (291.80 K) in 1997. Rivers and lakes often have a higher silt content than oceans. This difference probably also has something to do with the increasingly serious water pollution problem in the Zhujiang Delta, where the waste water resulting from sugar refining, paper pulp processing, textile dyeing and electroplating is often directly released into rivers (Lin 1997). Forests show a considerably low radiant temperature in both years, because dense vegetation can reduce amount of heat stored in the soil and surface structures through transpiration. However, forests show a relatively large standard deviation in radiant temperature values (9.37 K in 1989 and 10.04 K in

1997) compared with other land cover types, indicating the heterogeneous nature of tree covers. Cropland, horticulture farms, and dike–pond land tend to have a sparse vegetation and exposed bared soil. The influence of surface soil water content and vegetation contribute to a broad variation in their surface radiant temperature value.

Given the relationship between surface radiant temperature and the texture of land cover that is influenced by land use, changes in land use and land cover can have a profound effect on the surface radiant temperature in a region. GIS coupled with image processing can help one to visualize the impact of land use and land cover change on surface radiant temperature. The technique of image differencing is employed to produce a radiant temperature change image after the surface radiant temperature of each year has been normalized. This image is then overlaid with the images of urban expansion. The results of GIS analysis show that the urban development between 1989 and 1997 has given rise to an average increase of 13.01 deg K in surface radiant temperature, with a standard deviation of ± 10.60 deg K. It should be noted that this number of increase could be applied to changed areas only.

4.2.2. *Relationship between radiant surface temperature and NDVI*

The relationship between surface radiance temperature and NDVI was investigated for each land cover type through correlation analysis (pixel by pixel). Table 6 shows the Pearson's correlation coefficients between the two elements in 1989 and 1997. The significance of each correlation coefficient was determined using a one-tail Student's *t*-test. It is apparent from table 6 that surface radiance temperature values tend to negatively correlate with NDVI values for all land cover types in both years. The highest negative correlation was found in forest (-0.8539) and urban or built-up land (-0.7731) in 1989, and in urban or built-up land (-0.9495) and forest (-0.8897) in 1997. In both years, horticulture farms exhibit a very significant correlation (-0.7569 for 1989 and -0.7966 for 1997). An even lower correlation was observed in construction sites of both years (-0.4549 and -0.3375).

The strong, negative correlation between surface radiance temperature and NDVI implies that the higher biomass a land cover has, the lower the surface temperature. Because of this relationship between surface radiance temperature and NDVI, changes in land use/cover have an indirect impact on surface temperatures through NDVI. The values of NDVI in each year were scaled according to the following formula (Gillies *et al.* 1997), because the absolute values of NDVI tend to vary temporally in a non-systematic manner (Price 1987, Che and Price 1992):

$$N^* = \frac{NDVI - NDVI_o}{NDVI_s - NDVI_o} \tag{5}$$

Table 6. Pearson's correlation coefficients between average surface temperature in degrees Kelvin and NDVI by land cover type (significant at 0.05 level).

Land cover	1989	1997
Urban or built-up land	-0.7731	-0.9495
Barren land	-0.4549	-0.3375
Cropland	-0.6320	-0.0971
Horticulture farms	-0.7569	-0.7966
Dike–pond land	-0.2756	-0.2588
Forest	-0.8539	-0.8897
Water	-0.1921	-0.1784

where $NDVI_o$ is the minimum value and $NDVI_s$ the maximum value of NDVI in an image. Usually, $NDVI_o$ is associated with 'water' while $NDVI_s$ is associated with 'forest'. Image differencing was then performed between the 1997 and 1987 NDVI images. GIS analysis indicates that the scaled NDVI value decreased 0.11 between 1989 and 1997 in the urbanized areas.

4.2.3. *Spatial distribution of surface radiant temperature*

The impact of land use and cover changes on surface radiant temperature can also be examined spatially. The surface temperature change image obtained by image differencing is recoded into eight temperature zones based on the classification scheme of equal interval. Zones 7 and 8 have a positive value of temperature change, indicating a temperature increase between 1989 and 1997, while others have a negative value. The mapped patterns of temperature change exhibit distinctly different spatial patterns among the eight temperature zones. A query regarding the areal extent and spatial occurrence of each zone indicates that the spatial pattern of zone 8 (Temperature increase = 24.25–48.5 K) (figure 4) coincides with that of urban expansion. A GIS analysis using buffer and overlay functions was conducted to acquire the density of temperature zone 8 in each 500 m buffer zone away from major roads. The result shows a tendency toward decreasing densities, as distance increases from roads. A correlation analysis between the density of temperature zone 8 and that of urban expansion gives a multiple r value of 0.6310 (significant at 0.05 level), thus leading to the conclusion that urban expansion is conducive to the increase in surface radiant temperature.

5. Discussions and conclusions

In this study, an integrated approach of remote sensing and GIS was developed for evaluation of rapid urban expansion and its impact on surface temperature in the Zhujiang Delta, China. Results revealed a notable increase in urban land use/cover between 1989 and 1997. Urban land development was uneven in different parts of the delta, and the density of urban expansion showed a tendency of decline as the distance increased away from a major road.

The combined use of remote sensing and GIS allows for an examination of the impact of urban expansion on surface temperature. The results showed that urban land development raised surface radiant temperature by 13.01 K. This study has also demonstrated that the direct effect of urban land use/cover change on one environmental element can cause indirect effect on the other. The increase of surface radiant temperature was related to the decrease of biomass.

The spatial pattern of radiant temperature increase was correlated with the pattern of urban expansion. This is particularly true when all these patterns were referenced to major roads.

The integration of remote sensing and GIS provides an efficient way to detect urban expansion and to evaluate its impact on surface temperature. The digital image classification coupled with GIS has demonstrated its ability to provide comprehensive information on the nature, rate and location of urban land expansion. Biophysical measurements including surface radiant temperature and biomass can be extracted from Landsat TM images. Using the technique of image differencing the environmental changes over time can be evaluated. To examine the environmental impact of urban expansion, the mapped patterns of environmental changes can be linked to urban expansion pattern by correlation analysis.

The environmental impacts of land use and land cover change can be modelled at local level using the integrated approach of remote sensing and GIS. The methodology employed in this study provides an alternative to the traditional empirical observation and analysis using *in situ* (field) data for environmental studies. This methodology should be possible to apply to other regions in China or in other nations that undergo a rapid urbanization. Future modelling efforts should test the possibility and feasibility that an integrated approach of remote sensing and GIS can be applied to investigate regional and global environmental impacts of land use and land cover change.

However, in applying the methodology used in this paper and the above finds, the following two points must be borne in mind. First, the computed surface radiant temperatures may be higher than as they were, since the effects of surface roughness on surface temperature have not been taken into account. Several authors (Kimes 1983, Cassels *et al*. 1992a, b) have elaborated this issue, and suggest scrutinizing the temperatures of each part of the vegetation–ground system (such as shaded ground, sunny ground, shade vegetation and sunny vegetation) and examining the effects of different canopy structures. Effective land surface temperature can be derived only after its relationship to the component temperatures has been mathematically modelled. Secondly, a more complicated emissivity correction scheme that differentiates seven types of land covers should be applied in any further study. Effective measurement of surface temperatures requests to analyse the significance of the nature of surface and its roughness on emissivities.

Acknowledgments

The author is grateful to Dr Chor Pang Lo for his help and suggestions on an early version of this paper. The funded support of the National Geographic Society, which made my fieldwork possible, is also greatly acknowledged. Last but not least, the author wishes to thank anonymous reviewers for their useful comments and suggestions.

References

Artis, D. A., and Carnahan, W. H., 1982, Survey of emissivity variability in thermography of urban areas. *Remote Sensing of Environment*, **12**, 313–329.

Balling, R. C., and Brazell, S. W., 1988, High resolution surface temperature patterns in a complex urban terrain. *Photogrammetric Engineering and Remote Sensing*, **54**, 1289–1293.

Carnahan, W. H., and Larson, R. C., 1990, An analysis of an urban heat sink. *Remote Sensing of Environment*, **33**, 65–71.

Cassels, V., Sobrino, J. A., and Coll, C., 1992a, On the use of satellite thermal data for determining evapotranspiration in partially vegetated areas. *International Journal of Remote Sensing*, **13**, 2669–2682.

Cassels, V., Sobrino, J. A., and Coll, C., 1992b, A physical model for interpreting the land surface temperature obtained by remote sensors over incomplete canopies. *Remote Sensing of Environment*, **39**, 203–211.

Che, N., and Price, J. C., 1992, Survey of radiometric calibration results and methods for visible and near infrared channels of NOAA-7, -9 and -11 AVHRRs. *Remote Sensing of Environment*, **50**, 1–7.

Department of Geography, Zhongshan University, 1988, *The Land and Water Resources in the Zhujiang Delta* (Guangzhou: Zhongshan University Press).

Ditu Chubanshe, 1977, *Provincial Atlas of the People's Republic of China* (Beijing: People's Press).

Ehlers, M., Jadkowski, M. A., Howard, R. R., and Brostuen, D. E., 1990, Application of

SPOT data for regional growth analysis and local planning. *Photogrammetric Engineering and Remote Sensing*, **56**, 175–180.

Gallo, K. P., McNab, A. L., Karl, T. R., Brown, J. F., Hood, J. J., and Tarpley, J. D., 1993a, The use of NOAA AVHRR data for assessment of the urban heat island effect. *Journal of Applied Meteorology*, **32**, 899–908.

Gallo, K. P., McNab, A. L., Karl, T. R., Brown, J. F., Hood, J. J., and Tarpley, J. D., 1993b, The use of a vegetation index for assessment of the urban heat island effect. *International Journal of Remote Sensing*, **14**, 2223–2230.

Gillies, R. R., and Carlson, T. N., 1995, Thermal remote sensing of surface soil water content with partial vegetation cover for incorporation into climate models. *Journal of Applied Meteorology*, **34**, 745–756.

Gillies, R. R., Carlson, T. N., Cui, J., Kustas, W. P., and Humes, K. S., 1997, A verification of the 'triangle' method for obtaining surface soil water content and energy fluxes from remote measurements of the Normalized Difference Vegetation index (NDVI) and surface radiant temperature. *International Journal of Remote Sensing*, **18**, 3145–3166.

Gong, Z., and Chen, Z., 1964, The soils of the Zhujiang River Delta. *Journal of Soils*, **36**, 69–124 (in Chinese).

Harris, P. M., and Ventura, S. J., 1995, The integration of geographic data with remotely sensed imagery to improve classification in an urban area. *Photogrammetric Engineering and Remote Sensing*, **61**, 993–998.

Jensen, J. R., 1996, *Introductory Digital Image Processing: A Remote Sensing Perspective*, 2nd edn (Upper Saddle River, NJ: Prentice Hall).

Kidder, S. Q., and Wu, H. T., 1987, A multispectral study of the St. Louis area under snow-covered conditions using NOAA-7 AVHRR data. *Remote Sensing of Environment*, **22**, 159–172.

Kimes, D. J., 1983, Remote sensing of row crop structure and component temperatures using directional radiometric temperatures and inversion techniques. *Remote Sensing of Environment*, **13**, 33–55.

Lin, G. C. S., 1997, Transformation of a rural economy in the Zhujiang Delta. *China Quarterly*, **149**, 56–80.

Lo, C. P., 1989, Recent spatial restructuring in Zhujiang Delta, South China: a study of socialist regional development strategy. *Annals of the Association of the American Geographers*, **79**, 293–308.

Lo, C. P., Quattrochi, D. A., and Luvall, J. C., 1997, Application of high-resolution thermal infrared remote sensing and GIS to assess the urban heat island effect. *International Journal of Remote Sensing*, **18**, 287–304.

Malaret, E., Bartolucci, L. A., Lozano, D. F., Anuta, P. E., and McGillem, C. D., 1985, Landsat-4 and Landsat-5 Thematic Mapper data quality analysis. *Photogrammetric Engineering and Remote Sensing*, **51**, 1407–1416.

Markham, B. L., and Barker, J. K., 1985, Spectral characteristics of the LANDSAT Thematic Mapper sensors. *International Journal of Remote Sensing*, **6**, 697–716.

Mather, A. S., 1986, *Land Use* (London: Longman).

Nemani, R. R., and Running, S. W., 1989, Estimation of regional surface resistance to evapotranspiration from NDVI and thermal-IR AVHRR data. *Journal of Applied Meteorology*, **28**, 276–284.

Nichol, J. E., 1994, A GIS-based approach to microclimate monitoring in Singapore's high-rise housing estates. *Photogrammetric Engineering and Remote Sensing*, **60**, 1225–1232.

Price, J. C., 1987, Calibration of satellite radiometers and the comparison of vegetation indices. *Remote Sensing of Environment*, **21**, 15–27.

Roth, M., Oke, T. R., and Emery, W. J., 1989, Satellite derived urban heat islands from three coastal cities and the utilisation of such data in urban climatology. *International Journal of Remote Sensing*, **10**, 1699–1720.

Ruddle, K., and Zhong, G., 1988, *Integrated Agriculture–Aquaculture in South China: the Dike–Pond System of the Zhujiang Delta* (Cambridge: Cambridge University Press).

Steffen, W. L., Walker, B. H., Ingram, J. S., and Koch, G. W., 1992, Global change and terrestrial ecosystems: the operational plan. IGBP Report No. 21, International Geosphere–Biosphere Programme, Stockholm.

Treitz, P. M., Howard, P. J., and Gong, P., 1992, Application of satellite and GIS technologies for land-cover and land-use mapping at the rural-urban fringe: a case study. *Photogrammetric Engineering and Remote Sensing*, **58**, 439–448.

Weng, Q., 1998, Local impacts of the post-Mao development strategy: the case of the Zhujiang Delta, southern China. *International Journal of Urban and Regional Studies*, **22**, 425–442.

Yeh, A. G. O., and Li, X., 1996, Urban growth management in the Pear River delta—an integrated remote sensing and GIS approach. *ITC Journal*, **1**, 77–85.

Zhong, G., 1980, The mulberry dike-fish pond system in the Zhujinag Delta: a man-made ecosystem of land–water interaction. *Acta Geographica Sinica*, **35**, 200–212.